Stability of the Superplastic Behavior of Glassy Polystyrene Thin Films in Sandwich Structures

C. H. Lin and A. C.-M. Yang*

Department of Materials Science and Engineering, National Tsing Hua University, Hsinchu, Taiwan

Received September 13, 2000; Revised Manuscript Received April 11, 2001

ABSTRACT: The development of crazes in thin films of glassy polymers is a result of a micronecking process. Hence, when sandwiched between ductile poly(phenylene oxide) (PPO) films, a brittle glassy polystyrene (PS) film can be plastically deformed to very large strains without crazing or cracking. However, the stability of this superplastic behavior is strongly dependent upon thickness of the outer ductile films. A sharp ductile−brittle transition in the sandwich thin film structure was observed as the PPO thickness decreased. A simple mechanical model built upon the competition between the necking force, associated with crazing, and the constraining force, due to the ductile films, was utilized to analyze the stability of this superplasticity. The result of the mechanical analysis is in good agreement with the experimental data. The mechanical calculation indicates that the constraining force from the outer layers should be at least 60 MPa greater than the necking force to ensure the superplasticity. The defect size corresponding to this excess constraining stress is around 18 nm, comparable in size of the correlation length of polystyrene chains.

1. Introduction

During stretching, a glassy polymer first deforms uniformly and elastically until it yields, which afterward deforms plastically.[1] The onset of plastic deformation can usually be detected by the deviation from the linear stress−strain curve or estimated theoretically by the critical yield criteria.[2,3] However, strong time and temperature dependence exists. Yielding in glassy polymers, however, remains intriguing in that the operating molecular mechanisms are still quite obscure. Although yielding may signify the start of ductile deformation, for most glassy polymers, the onset of plastic deformation is usually equivalent to that of strain localization from which cracking and fracture originate. Crazing and local shear deformation[4−12] are the two types of strain localization found in glassy polymers. Crazes, commonly observed in deformed brittle polymers, e.g., polystyrenes, are cracklike defects that are load-bearing and feature a fibrilous microstructure.[4−26] On the other hand, local shear deformation is commonly regarded as the ductile counterpart of crazing; the degree of strain localization is much less compared to crazing. Because the shear deformation zones are uniformly thinned intact films instead of the fibrilous microstructure made of chain-scissioned polymer,[7,13,14,17,18,23] they withstand a much greater stress before fracture.

Because of its importance in both academia and practical applications, the pursuit of the underlying mechanisms operative during crazing and shear yielding has never diminished since the 1960s.[4−26] Among others, distinguished contributions have been accomplished by Kambour[4] and Kramer.[7,9,11−14,20,23−25] It has been concluded that crazing is a result of surface drawing which is preceded by the appearance of locally stress-softened spots. The stress-softened spots then open up following a meniscus instability and then merge together, demonstrating a so-called fingers growth pattern[7,20−23] that eventually leads to the development of craze fibrils. By surface drawing, new material is drawn from the bulk into the thin "active zones" at the craze/bulk boundaries. At the active zone, the drawn material is strain softened and becoming fully drawn fibrils when it subsequently exits and enters into the craze. The extraordinarily large extension ratio of the fibrils, measured by TEM microdensitometry,[9,10] is attributed to the large extension of the molecular network, during which, a large degree of chain disentanglements and chain scissions occur.[7,14,18,23−25] Later, Yang et al. used the atomic force microscopy (AFM) method and discovered that crazing is, in fact, a result of micronecking, a mechanism very similar to one operative during local shear deformation.[15−16] The surface of the craze is not only drawn but also depressed in a fashion identical to necking.[1,15,17,26−28] Crazing and local shear deformation, however, follow quite distinct molecular mechanism. It has been revealed that crazing is associated with significant chain network extension that strongly depends on the entanglement density, whereas local shear involves only limited but constant local network deformation.[17]

Nevertheless, any form of strain localization always reduces material toughness. Since crazing, or local deformation, follows a micronecking mechanism, a remarkable increase of ductility should result if micronecking can be suppressed. There have been many attempts to explore these possible toughening mechanisms for glassy polymers.[29−40] One prominent approach involves compounding small rubber particles into the glassy polymer, thus producing the effect of enhancing the initiation, but restricting the growth and breakdown of crazes at the same time. An example of this approach is the high impact polystyrene (HIPS). Another interesting approach is the multilayer co-extrusion process. In one example, a laminate product composed of hundreds of alternating SAN and PC ultrathin films (Dow Chemicals Co.) demonstrates amazingly superior mechanical ductility. The mechanical properties of these multilayer systems have been studied in detail by Baer

* Corresponding author. E-mail: ACYANG@MSE.NTHU.EDU.TW.

10.1021/ma001586c CCC: $20.00
Published on Web 06/09/2001

et al.[32−37] They discovered that as the number of ultrathin layers increases, the toughness of the multilayer system increases whereas the fracture mode in the brittle SAN layers shifts from crazing to shear deformation. The toughening effect in other laminated structures was also studied by Umemoto et al.[38,39] Furthermore, increasing cross-linking density in brittle polymers was found to have an effect in triggering the transition of fracture mode from crazing to shear deformation.[25,40] These toughening methods, however, did not provide solutions for complete elimination of any strain localization, nor simple insights into effective manipulation of the development of local deformation zones. On the basis of the micronecking observation, one would expect that crazing, or shear deformation, could be completely "switched off" if the necking force is overcome by, for example, a constraining force. Hence, a sandwich trilayer structure containing a brittle polymer in the middle layer was deviced to test this approach. Excellent superplasticity results were obtained.[19] The toughness of the brittle polymer increased dramatically, and strain localization was completely eliminated, even at very large strains (> 20%). The stability of this superplastic behavior was further analyzed using the Bridgman plasticity[41] and the plate deflection theory.[42] Good agreement was achieved between the result of mechanical analysis and the experimental observations.

2. Experimental Procedures

The trilayer structures were prepared by stacking two poly(2,6-dimethyl-1,4-phenyl oxide) (PPO) films above and beneath a polystyrene (PS) film. The PPO was purchased from Aldrich Chemical Co. with M_w and M_n being 244 000 and 32 000, respectively. The PS is monodisperse ($M_w/M_n = 1.3$; Pressure Chemicals Co.) with $M_w = 2$ M. Each film was prepared by solution cast from the toluene solution of the polymer. The laminated structure was prepared by first transferring a PPO film onto a piece of ductile copper grids, and then sequentially stacking a PS film and then a second PPO film on top of it.[9] The copper grids have a thickness of approximately 0.20 mm, and the size of each grid square is approximately 1 mm. The grid bars were dip-coated with a thin layer of polymer film before film stacking. For better adhesion between polymer films and more reliable polymer/grid bars bonding, the trilayer samples were kept in toluene vapor for a short period of time (a few seconds). The samples were then stored overnight in ambient conditions to remove any residual solvent. According to FTIR analysis, the residual solvent in the prepared samples is negligible.[12] The details of the film stacking technique on copper grids can be found in the publications of Kramer.[7,9,11−14,19,22−24]

The samples were then mounted in a manual strain jig and stretched, with a strain rate restricted within the range of $10^{-4}-10^{-5}$/s.[43,44] The critical strain of crazing was determined statistically by in situ monitoring with an optical microscope during tensile deformation.[13] The deformation zones were further examined by using an AFM (Digital Instruments, Nanoscope IIIA) to investigate the topography of the strain localization regions. The degree of strain localization (DSL) of the stretched sample was determined by directly measuring the total width of the deformation zones in each film square perpendicular to the stretching direction[19] with a 500× optical microscope and a LECO 2000 digital image analysis system.[19]

3. Results and Discussions

3.1. The Mechanical Behavior of Free-Standing Films. Upon stretching, crazes nucleate in the free-standing PS film (single layer) from the edges of film squares or local defects such as dust particles, shown in Figure 1. The crazing strain ϵ_c of the 0.1 μm thick free-standing PS film was around 0.9%, independent of film thickness. It is worth noting that at a 10% strain, almost all crazes were grown to cross the entire film squares. The degree of strain localization (DSL), a quantitative measure of strain localization, is defined as the ratio between the strain concentrated in crazes to that being applied.[19] The DSL in the single layer PS film is very close to zero for $\epsilon < \epsilon_c$ (=0.9%), but it increases dramatically to 100% as the applied strain $\epsilon > 5\%$. This result indicates that when crazes develop in the PS film, nearly all the deformation is concentrated into the crazed areas and that the uncrazed matrix is subjected to no further strain beyond ϵ_c.

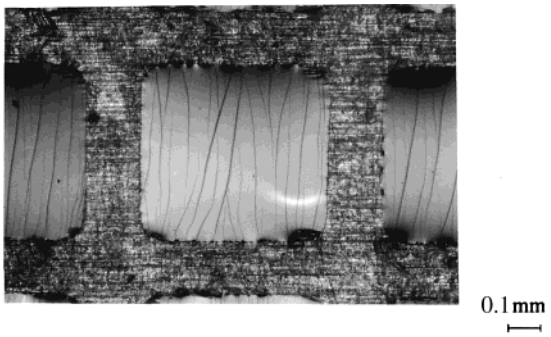

Figure 1. Optical micrograph of the crazed 0.1 μm thick PS film supported on the copper grids at 10% strain.

The crazed region in the stretched PS film was examined further by using AFM. The AFM surface profile of a typical craze is shown in Figure 2. The depth of the conspicuous surface depression in the craze increases linearly with craze width w until a maximum depth w_c is reached, after which the surface depression levels off (shown in Figure 3). This is very similar to neck propagation in the cold drawing process of semicrystalline polymers; hence it was termed micronecking for crazing. The slope α of the neck shoulder, the critical width w_c at which the depth starts to level off, and the maximum depression depth d_m are important parameters for analyzing the micronecking process. For 0.1 μm thick PS thin films, the slope $\alpha = 20.1°$, the critical width $w_c = 1000$ nm, and the maximum depth $d_m = 35$ nm are listed in Table 1.

On the other hand, the fresh PPO thin films were found to deform uniformly without strain localization up to more than 20% strain. Only when aged (ambient conditions for more than 1 week) or annealed at high temperatures (160−200 °C, 1 h) did the PPO films begin to show prominent local shear deformation zones upon stretching.[12] Therefore, the fresh PPO films were used to laminate the PS film into a trilayer structure for studying the superplastic behavior of the sandwiched brittle polymers. To ensure uniform deformation, all PPO samples were used and tested within 5 days of sample preparation.

3.2. The Superplastic Behavior of the Sandwiched Film. As clearly shown, craze formation follows micronecking mechanics.[15,17] Therefore, if nucleation of micronecking was inhibited, crazing of the brittle film would consequently be depressed. A trilayer structure is prepared by sandwiching the brittle PS film between two ductile fresh PPO films, so that the depression due to micronecking in PS during tensile deformation is

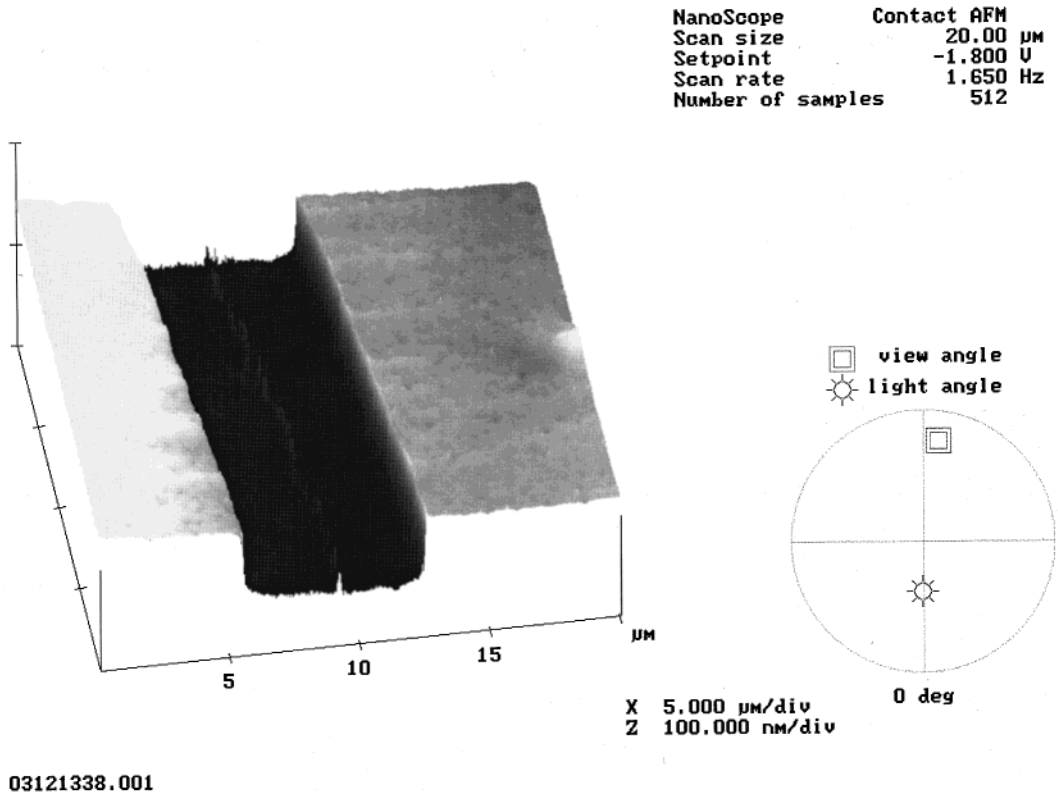

Figure 2. AFM topography of a craze in the 0.1 μm thick PS film.

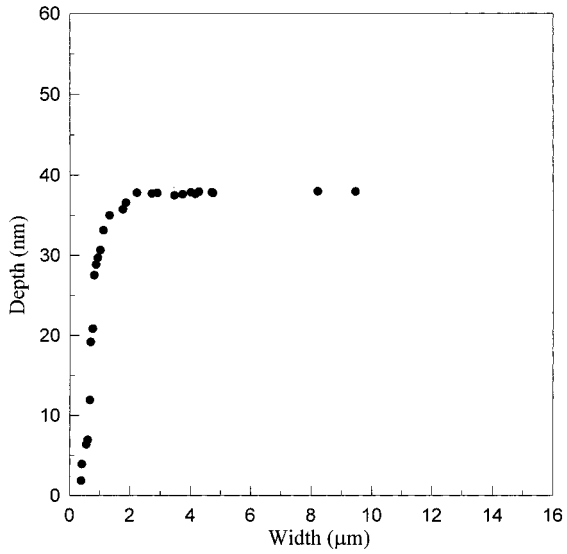

Figure 3. Depth vs width of the craze depression in a 0.1 μm thick PS film.

strongly constrained by the outer uniformly deformed PPO films. For convenience in this discussion, the trilayer structure is designated as $h_1/h_2/h_1$ where h_1 and h_2 are, respectively, the thicknesses in micrometers of the PPO and PS films. As revealed by the experimental data, strain localization in polymer films indeed could be "switched off" in these sandwich structures. As a demonstration, the trilayer structure 0.5/0.1/0.5 (Figure 4f) showed no local deformation zones under large strains far more than the critical strain ($\epsilon_c = 0.9\%$) of PS films. Any strain localization in the PS film could be easily detected under the optical microscope since the PPO films are transparent. During the entire tensile deformation up to 20% strain, at which point the supporting copper grids eventually broke, the PS film

Table 1. Necking Parameters Measured by AFM for the Deformation Zones in the Sandwich Thin Film Structures

	depression depth at the neck, d_m, nm	slope of the neck shoulder, α, deg	critical width of the neck, w_c, nm
0.1 μm PS	35	20.1	1000
0.05 μm PPO/0.1 μm PS/0.05 μm PPO	80	2.3	2000
0.1 μm PPO/0.1 μm PS/0.1 μm PPO	90	1.2	4500
0.2 μm PPO/0.1 μm PS/0.2 μm PPO	100	0.9	6000

always deformed uniformly. This outstanding superplastic behavior of the brittle PS polymer in the trilayer structure illustrates that if the micronecking was depressed, so would crazing and any other similar forms of strain localization.

The superplastic behavior of the trilayer structure is strongly dependent on the PPO film thickness h_1. When h_1 is small, the superplastic behavior diminishes. The effect of the PPO thickness on the degree of strain localization (DSL) is shown in Figure 5 where a ductile−brittle transition was observed at approximately $h_1 = 0.3\ \mu$m. For $h_1/0.1/h_1$ trilayers with h_1 less than 0.3 μm, extensive local deformation zones still appear upon stretching and the crazing strain ϵ_c is quite close to that of the free-standing PS films. These deformation zones (shown in Figure 4, part a−f), however, were remarkably different from those of the ordinary crazes in the free-standing PS films. The growth of the deformation zones was highly suppressed such that they grew into short whiskerlike shapes. The degree of strain localization (DSL) of these trilayer structures increases linearly with the applied strain[19] to only around 80% at $\epsilon = 20\%$. In sharp contrast, the DSL of the crazed free-standing PS films increases rapidly with strain, to very close to 100% soon after crazing. It indicates that although local

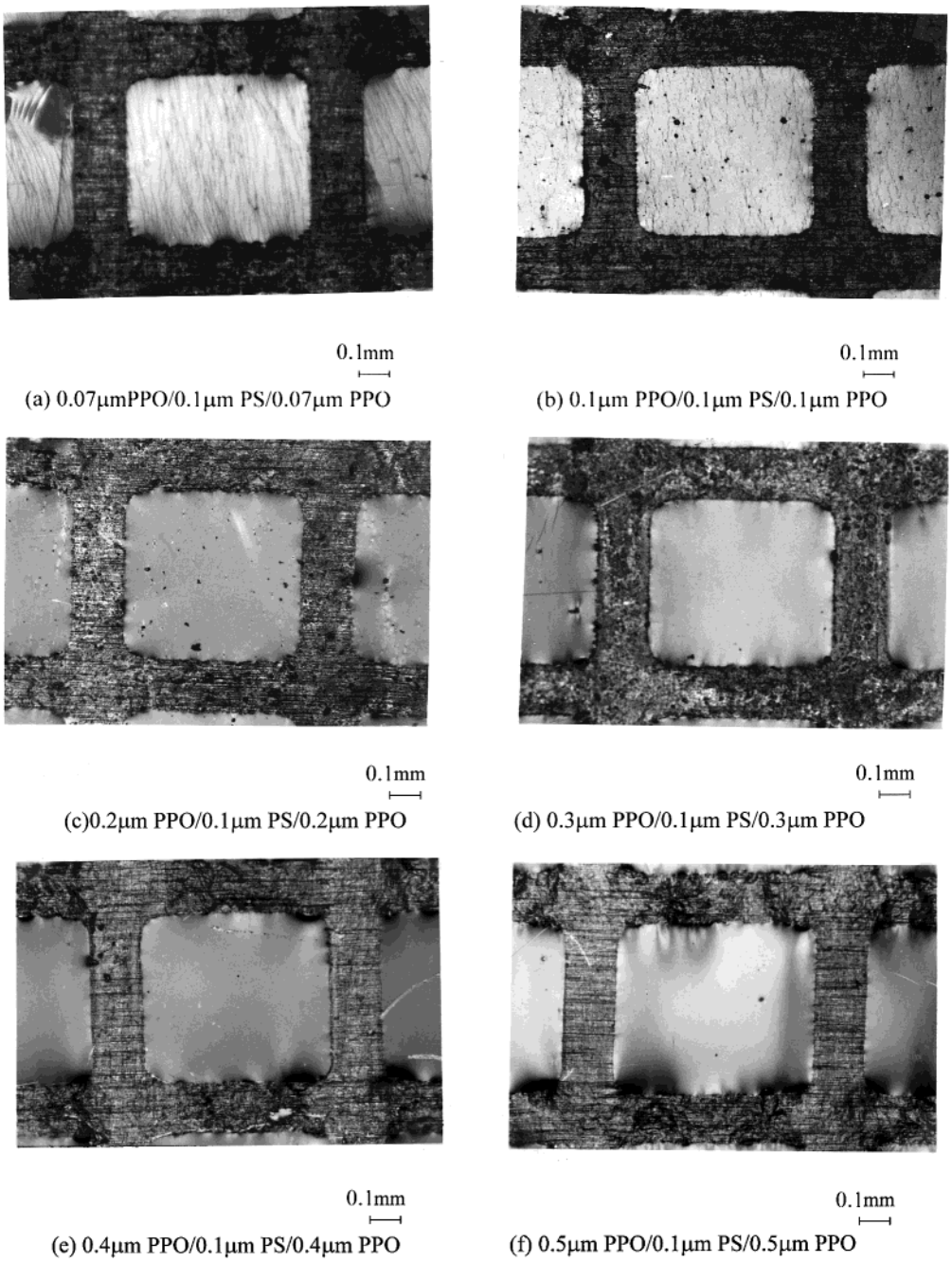

Figure 4. Optical micrographs of the strained trilayer sandwich thin film structures at 10% strain: (a) 0.07 μm PPO/0.1 μm PS /0.07 μm PPO, (b) 0.1 μm PPO /0.1 μm PS /0.1 μm PPO, (c) 0.2 μm PPO /0.1 μm PS /0.2 μm PPO, (d) 0.3 μm PPO /0.1 μm PS /0.3 μm PPO, (e) 0.4 μm PPO /0.1 μm PS /0.4 μm PPO, and (f) 0.5 μm PPO /0.1 μm PS /0.5 μm PPO.

deformation occurs in the trilayer structures where h_1 is less than 0.3 μm, the uncrazed matrix still bears a significant portion of the applied strain, contributing significantly to the fracture toughness of the sandwich structures. The local deformation zones in the trilayer structure were further examined by AFM; the measured data are listed in Table 1. The slope α of the neck shoulder of the local deformation zones decreased dramatically when the PS was sandwiched by the PPO films. The slope α also decreased further with increasing thickness h_1 of the PPO films. For the 0.2/0.1/0.2 structure, α is equal to 0.9°; it is conceivable that α approaches zero for greater h_1, and should eventually diminish for $h_1 > 0.3$ μm where superplasticity prevails. Furthermore, the critical width w_c and the depression depth d_m increased with PPO film thickness. From the depth data in Table 1, it is clear that the total depth of depression in the trilayer was greater than the PS film thickness, indicating that the PPO films also undergo necking as local deformation occurs in the trilayer.

For h_1/0.1/h_1 trilayers with h_1 greater than 0.3 μm, the crazes are very tiny and hard to detect. When h_1 becomes greater than 0.4 μm, any forms of strain localization were depressed. This observation indicates that the growth of local deformation zones in the brittle film sandwiched within the trilayer is indeed strongly constrained by the outer layers. When the outer layers are thick enough local deformation can be completely switched off, resulting in superplasticity of the brittle film.

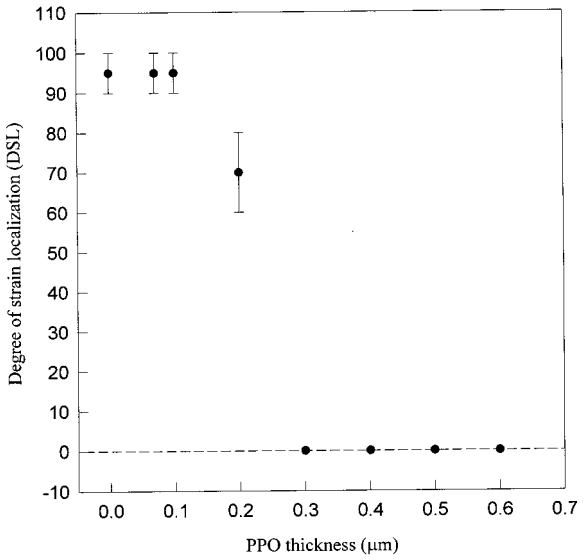

Figure 5. Degree of strain localization (DSL) of the trilayer sandwich thin film structures vs the thickness of the PPO outer layer. (applied strain = 10%).

To sustain the superplasticity, the necking force in the brittle film present when $\epsilon > \epsilon_c$ (PS) should be overcome by the constraint forces provided by the outer PPO layers. This requires that the PPO layers are thick enough and that the bondings between the PS and PPO films are strong enough to ensure effective stress transfer from the PPO layers to the PS layer. Once poor adhesion exists, local delamination would proceed, rendering the constraint force ineffective, and resulting in the dominance of the micronecking process. This factor, however, can be safely ruled out, as the secondary ion mass spectroscopy (SIMS)[19,45,46] data illustrates that there is always some limited extent of interdiffusion across the PPO/PS interfaces, ensuring good interfacial bonding.[19] Since the constraint force due to deflection of the outer films increases with the third power of the film thickness,[42] necking will dominates whenever the PPO film thickness is too thin. In the following section, the stability of PS superplasticity is examined from this approach.

3.3. Mechanical Stability of the Superplasticity in the PS Film. Before carrying out the mechanical analysis, some considerations have to be first cleared. In the tensile experiments here, the polymer film was deformed by stretching the supporting copper grids that were well bonded to the polymer film. The transfer of strain (or strain energy) from the copper grids to the polymer film, primarily due to good bonding, was found to be quite effective. For the purpose of bonding enhancement, the grid bars were precoated with a thin layer of polymer before the polymer film deposition and, after film deposition, immersed in the toluene vapor to trigger cross-interface diffusion. Furthermore, the polymer film, when deposited on the copper grids, was effectively divided into mechanically independent film squares by the bonding grid bars. The maximum variation of strain in the through-thickness direction was estimated to be less than 0.015%. Therefore, the through-thickness stress and strain distribution in the polymer film was assumed to be constant. This assumption will not have an effect on the superplastic observation; it only simplifies the mechanical analysis of the superplasticity.

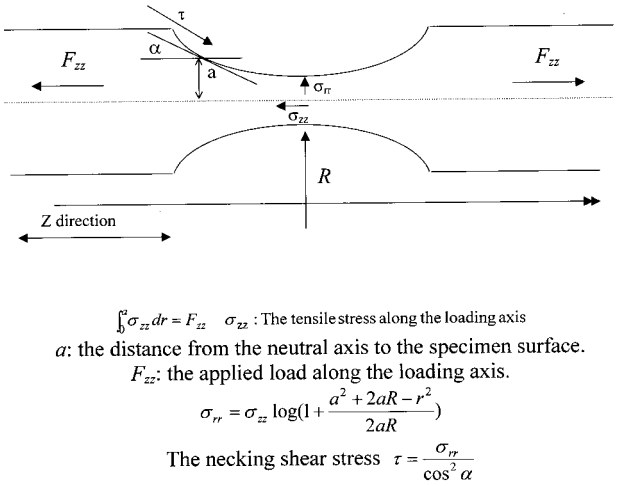

Figure 6. Schematic cross section of a crazing neck.

The superplasticity in the trilayer structure can be regarded as a competition between the necking force of the PS layer and the constraining bending force of the outer PPO layer caused by local film deflection. According to Bridgman,[12,15−17,19,41] a triaxial tension stress σ_{rr} and a shear stress τ are induced in the necked region schematically depicted in Figure 6. The hydrostatic tension σ_{rr} can be expressed as

$$\sigma_{rr} = \sigma_{zz} \log[1 + (a^2 + 2aR - r^2)/2aR]$$

where σ_{zz} is the applied tensile stress along the loading axis, a and r are the distances from the neutral axis in the specimen to the specimen surface and to the spot of consideration, respectively, and R is the local radius of curvature at the neck. The tensile stress σ_{zz} should satisfy the force balance boundary condition that $\int_0^a \sigma_{zz} dr = F_{zz}$, where F_{zz} is the applied load along the tensile axis. The induced shear stress τ at the surface of neck region is expressed as

$$\tau = \sigma_{rr}/\cos^2 \alpha$$

where α is the angle between the tangential plane and the tensile axis at the surface point of consideration. It is the shear stress τ that draws new materials from the matrix into craze to thicken the crazed region. Therefore, the shear stress τ is assumed to be the necking stress responsible for strain localization. The AFM surface profile of the craze can provide these geometric parameters to help calculate the necking stress τ of the micronecking process.

The local film deflection stress, on the other hand, can be estimated from the plate theory. According to Timoshenko,[42] a plate can be divided into many parallel beams and the mechanical behavior of the plate can be regarded as the superposition of that of each individual beam constrained under the appropriate boundary conditions. Let the vector **x** be the direction parallel to the beam length, and the vector **z** be the direction perpendicular to the plane of the plate. For a small plane deflection w in the z direction in a beam of length l, the strain ϵ_x at a distance z from the middle neutral surface is

$$\epsilon_x = -z \, d^2w/dx^2 \quad (1)$$

The strains ϵ_x and ϵ_y can be expressed in terms of the

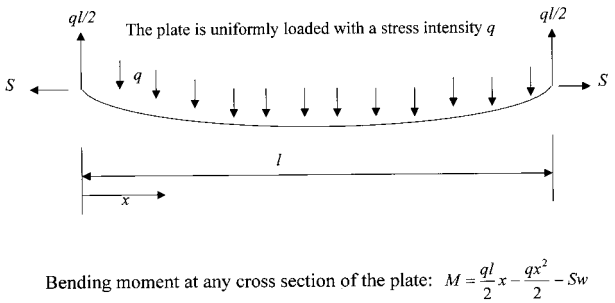

Figure 7. Cross section of a uniformly loaded elemental plate under the action of an axial force *S*.

normal stresses σ_x and σ_y to be

$$\epsilon_x = \frac{\sigma_x}{E} - \frac{\nu\sigma_y}{E}$$

$$\epsilon_y = \frac{\sigma_y}{E} - \frac{\nu\sigma_x}{E} \quad (2)$$

by assuming linear elasticity. Since the lateral strain ϵ_y must be zero to satisfy the continuity requirement in the plate during bending, the bending strain ϵ_x and stress σ_x become

$$\epsilon_x = (1 - \nu^2)\sigma_x/E$$

and

$$\sigma_x = \frac{E\epsilon_x}{1 - \nu^2} = -\frac{Ez}{1 - \nu^2}\frac{d^2w}{dx^2} \quad (3)$$

Furthermore, the bending moment of the elemental beam, by definition, is

$$M = \int_{-h/2}^{h/2} \sigma_x z \, dz = -\int_{-h/2}^{h/2} \frac{Ez^2}{1 - \nu^2}\frac{d^2w}{dx^2} dz = -\frac{Eh^3}{12(1 - \nu^2)}\frac{d^2w}{dx^2}$$

or

$$D\frac{d^2w}{dx^2} = -M \quad (4)$$

where $D \equiv Eh^3/12(1 - \nu^2)$. Equation 4 describes the relation between deflection w and bending moment M for a general plate. Now, consider a more specific case where a long rectangular plate is under a uniform load q and submitted to the action of an axial force S to the support, as depicted in Figure 7. Although the necking stress in the sandwiched PS film is not completely uniform, for simplification, the uniform load approximation is adopted here. The bending moment at any cross section of this plate is given as[42]

$$M = \frac{ql}{2}x - \frac{qx^2}{2} - Sw \quad (5)$$

Substitution of eq 5 into the eq 4 yields the following differential equation of the beam deflection w

$$\frac{d^2w}{dx^2} - \frac{Sw}{D} = -\frac{qlx}{2D} + \frac{qx^2}{2D} \quad (6)$$

The general solutions of eq 6 are of the following form

$$w = C_1 \sinh\frac{2ux}{l} + C_2 \cosh\frac{2ux}{l} + \frac{ql^3x}{8u^2D} - \frac{ql^2x^2}{8u^2D} - \frac{ql^4}{16u^4D} \quad (7)$$

where the parameter u is defined as

$$u^2 \equiv \frac{Sl^2}{4D}$$

The constants C_1 and C_2 in eq 7 determined from the boundary conditions that the deflection w at the both ends is zero, i.e., $w(x = 0) = 0$ and $w(x = l) = 0$, are

$$C_1 = \frac{ql^4}{16u^4D}\frac{1 - \cosh 2u}{\sinh 2u}$$

and

$$C_2 = \frac{ql^4}{16u^4D}$$

Hence, the deflection w of the plate can be expressed as

$$w = \frac{ql^4}{16u^4D}\left[\frac{\cosh u(1 - 2x/l)}{\cosh u} - 1\right] + \frac{ql^2x}{8u^2D}(1 - x) \quad (8)$$

The primary interests for considering the superplastic stability are the maximum force q_m, maximum deflection w_m, and the maximum bending moment M_m located at the middle of the strip. The maximum deflection w_m and the maximum bending moment M_m can be obtained from eq 8 and eq 5

$$w_m = \frac{5ql^4}{384D} f_0(u)$$

where

$$f_0(u) \equiv [(\text{sech } u - 1 + u^2/2)/(5u^4/24)]$$

$$M_m = \frac{ql^2}{8}\psi_0(u)$$

where

$$\psi_0 = (1 - \text{sech } u)/\left(\frac{u^2}{2}\right)$$

where the functions f_0 and ψ_0 both approach to 1 at the large u limit for the simple support cases where the tensile action at the beam ends can be ignored.[42] The large u limit is a reasonable assumption for the trilayer systems studied here because the PPO films are very thin compared to the lateral dimension of the film squares. Hence, the maximum deflection w_m and maximum bending moment M_m are

$$w_m = 5q_m l^4/384D$$

and

$$M_m = q_m l^2/8$$

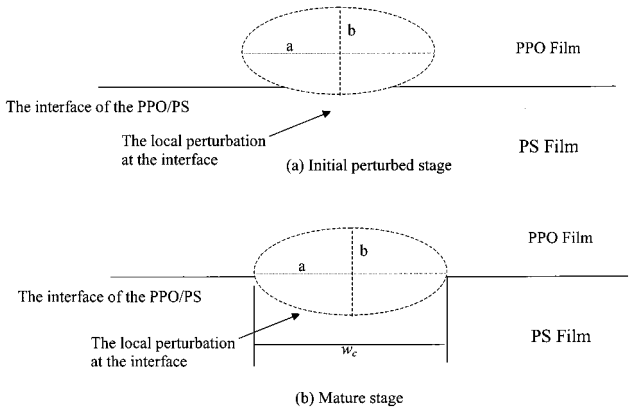

Figure 8. Configuration of the incipient elliptical corrugation at the strain-softened unstable area.

Subsequently, the maximum constraint force can be expressed as

$$q_m = 384Dw_{max}/5l^4$$

To calculate the necking stress and the restraining deflection force at the incipient strain localization, the shape of the primordial strain softened spots, which eventually lead to meniscus instability and fingers growth of crazes,[7,20−23] was approximated as a partial elliptical arc, as shown in Figure 8. As strain localization proceeds further, the corrugated and softened area grows both in depth and width, hence the elliptical arc length increases corresponding to the area growth. To simulate the AFM craze profile in a 0.1 μm thick PS film (Table I),[16,17] the ellipse is given with a long axis a = 500 nm and short axis b = 35 nm. With this profile, the drawing stress at every point on the corrugated area can be calculated from the curvature using the Bridgman model. The radius of curvature ρ of the elliptical profile $\vec{R}(s) = x(s)\vec{i} + y(s)\vec{j}$ can be expressed as[47]

$$\rho^{-1} = [|R'|^2|R''|^2 - (R'\cdot R'')^2]^{1/2}/|R'|^3$$

where R' and R'' are the first and second-order derivatives of $R(s)$ with respect to s which is the trajectory index parameter. By definition, the elliptic profile $R(s)$ is

$$\vec{R}(s) = s\vec{i} + \frac{b}{a}(a^2 - s^2)^{1/2}\vec{j}$$

whereas the radius of curvature becomes

$$\rho^{-1} = \frac{(1+K^2)\left(\frac{K}{s} + \frac{a^2K^3}{b^2s}\right)_2 - \left(\frac{K}{s} + \frac{a^2K^3}{b^2s}\right)^2 K^2}{(1+K^2)^{3/2}}$$

where

$$K \equiv \frac{b}{a}s(a^2 - s^2)^{-1/2}$$

The necking stress calculated using the Bridgman's equation and the elliptical simulation is shown in Figure 9. It is clear that as the corrugated depth increases, the necking stress first increases gradually. When the corrugated depth becomes close to the limiting value b, which, in fact, is the plateau depth of a mature craze, the necking stress increases dramatically. On the other

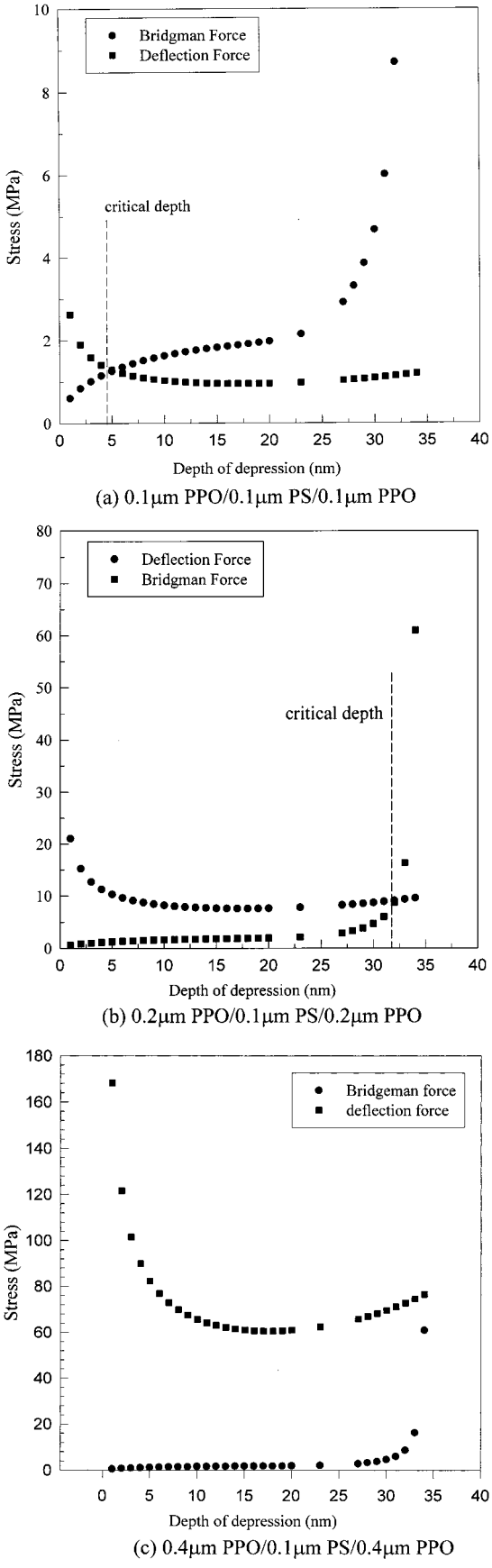

Figure 9. Competition of the drawing shear force and the deflection force in the trilayer structures: (a) 0.1 μm PPO/0.1 μm PS/0.1 μm PPO, (b) 0.2 μm PPO /0.1 μm PS /0.2 μm PPO, and (c) 0.4 μm PPO /0.1 μm PS /0.4 μm PPO.

hand, the maximum deflection force q_m of the outer PPO films calculated using the same elliptical profile with the plate theory derived above is also shown in Figure 9. The deflection force q_m is very high for very small corrugated depth, but decreases significantly and then levels off as the corrugated depth increases. From the relationship $q_m = 384Dw_{max}/5l^4$ where $D = Eh^3/12(1 - \nu^2)$, the constraint force increases to the third power of the PPO film thickness h_1. Therefore, increasing the thickness of the PPO films is an effective way to increase stability of superplasticity of the trilayers.

The competition of the two forces as a function of the corrugated depth (depression depth) is shown in Figure 9, parts a−c. Since only the data obtained during the incipient strain localization are useful for considering the outcome of competition between the necking force and the deflection force, the data of the large depth regime are of limited meaning here and consequently are ignored. For PPO thickness $h_1 = 0.1\ \mu$m, the necking force τ begins to overpower the constraint force q_m when a unstable region reaches a critical corrugated depth d_c as small as 5 nm. This result strongly implies that superplasticity is very unstable, since defects or intrinsic heterogeneities in the multilayers, if any, can easily produce a perturbation comparable to that size. For h_1 equal to 0.2 μm, the critical corrugated depth d_c increases to 30 nm. Although the fact that d_c is very close to the limit value b implying stable superplasticity, the difference of $(\tau - q_m)$ for $d > d_c$ is only approximately 7 MPa, indicating that a defect capable of inducing enough perturbation can destabilize the superplasticity. For $h_1 = 0.4\ \mu$m, the critical depth d_c increases further to around 35 nm, but the constraint force is also significantly greater than the necking force by a difference of 60 MPa, indicating a very stable superplasticity. As shown in the observed data, it is difficult to induce a mechanical instability of that magnitude, and even if strain localization was triggered, subsequently, the local stress relaxes while the perturbation decreases, and superplasticity again prevails. The short whiskerlike local deformation zones sporadically observed in the trilayers 0.4/0.1/0.4 apparently were produced in accord with this effect. Clearly, as h_1 increases further, strain localization is completely switched off as shown in Figure 4f. Figure 10 shows the critical depth d_c vs PPO film thickness indicating a ductile−brittle transition at around 0.2 μm, a transition very similar to that of the degree of strain localization DSL. Hence, the gap of 60 MPa in the case of $h_1 = 0.4$ is considered to be the lower limit of the difference $(q_m - \tau)$ required for superplasticity.

3.4. Estimation of the "Defect" Size in the Sandwiched Glassy Polymer Film. The stability of the superplastic behavior of the PS film, undoubtedly, is strongly influenced by the presence of defects. The defects create triaxial tension in the film favoring strain localization. For the purpose of analysis, the defects of the brittle film sandwiched in the trilayer structure are assumed to be a form of spherical inclusions. The local stress concentration $\tau'(c)$ around a spherical inclusion is given as[48]

$$\tau'(c,\theta)/\sigma_{zz} = 1 + 5[(1 + 3\cos 2\theta)/4]\,(\delta/c)^3$$

where σ_{zz} is the uniformly applied stress, δ is the size of the inclusion, and c and θ are the distance and angle of the location of consideration relative to the center of the inclusion. For the maximum stress conditions, let $\theta = 0$; hence the last equation becomes

$$\tau'(c)/\sigma_{zz} = 1 + 5(\delta/c)^3$$

or equivalently

$$\delta = c[\tau'(c)/\sigma_{zz} - 1]/5]^{-1/3}$$

It is assumed that, during the superplastic deformation, the stress σ_{zz} in the sandwiched PS film is very close to that of crazing in the free-standing PS film, i.e., $\sigma_{zz} = E\cdot\epsilon_c$ = (3200 MPa)(0.01) ≒ 30 MPa, where E is the Young's modulus of PS. When the local stress concentration τ' reaches 60 MPa, the induced mechanical perturbation triggers strain localization, hence

$$\delta \doteqdot c/\sqrt[3]{5}$$

For approximation, let c be the critical corrugated depth d_c of the incipient neck (30 nm), and the defect size δ becomes

$$\delta \doteqdot 18\ \text{nm}$$

very close to the correlation length ξ (or equivalently the entanglement network spacing) in PS reportedly to be around 10 nm.[7,49] Hence, for the trilayer systems with thin PPO films (h_1 < approximately 0.4 μm), it is likely impossible to achieve superplasticity by further removing dust particles or by improving sample preparation technique. Although more experiments are needed to delineate the relationship between the correlation length ξ and δ, if ξ indeed is the lower limit of affine deformation, polymer films with the greater correlation length would require thicker ductile outer-layer films to stabilize superplasticity. The mechanical model offers a good insight and prediction of mechanical stability of superplasticity in multilayer systems. The effect of defects on the superplastic behavior can be analyzed from the consideration of this mechanical model.

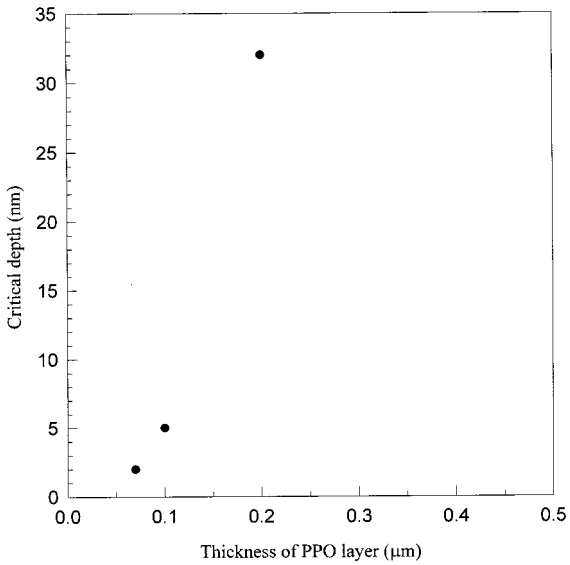

Figure 10. Critical depth d_m of the incipient unstable area in the trilayer structure versus the thickness of the PPO outerlayer.

4. Conclusions

The following conclusions may be made.

1. A brittle polymer thin film can clearly demonstrate superplastic behavior when sandwiched between ductile outer layers of polymers. That is, the brittle polymer can be deformed uniformly up to very large strains (>20%) without forming any type of strain localization. This effect is strongly dependent on the thickness of the outer layer films. However, when the outer layer films are too thin, strain localization would proceed. In a PPO/PS/PPO system, a brittle−ductile transition was observed when the outer PPO film thickness was at 0.3 μm for a 0.1 μm thick PS film. The deformation zones in the sandwiched layers show a retarded growth, and the degree of strain localization data indicates that the matrix film still bears a significant portion of the applied strain.

2. The stability of the superplasticity of the sandwiched brittle polymer can be analyzed by considering the competition between the necking force that favors strain localization and the film deflection force resisting strain localization due to the outer layers. Good agreement was obtained with the experimental results. The mechanical calculation indicates that the constraining force from the outer layers should be at least 60 MPa greater than the necking force to ensure superplasticity. Since the film deflection force increases to the third power of the film thickness, increasing the outer layer thickness is an effective way to stabilize superplasticity.

3. The 60 MPa difference between the two forces at the brittle−ductile transition was used to estimate the size of defects that incite the formation of the incipient strain localization. The size of defect was estimated to be around 18 nm, in the same order of magnitude of the correlation length of the PS film. The correlation length is possibly the lower bound of affine deformation in glassy polymers.

Acknowledgment. We greatly appreciate the financial support by the National Science Council of Taiwan. We also appreciate the ever-lasting inspirations and encouragements from the instructions by Prof. E. J. Kramer and Dr. H. R. Brown. The assistance by Mr. W. C. Chen of our laboratory in NTHU in the AFM experiments is also greatly appreciated.

References and Notes

(1) Ward, I. M. *Mechanical Properties of Solid Polymers*, 2nd ed.; John Wiley & Sons Press: New York, 1983.
(2) Tresca, H. *C. R. Acad. Sci. Paris* **1867**, *64*, 809.
(3) Coulomb, C. A. *Mèm. Math. Phys.* **1773**, *7*, 343.
(4) Kambour, R. P. *J. Polym. Sci. Macromol. Rev.* **1973**, *7*, 1.
(5) Rabinowitz, S.; Beardmore, P. *CRC Rev. Macromol. Sci.* **1972**, *1*, 1.
(6) Gent, A. N. *The Mechanics of Fracture AMD*; ASME: New York, 1976; Vol. 19, p 55.
(7) Kramer, E. J. *Adv. Polym. Sci.* **1983**, *52/53*, 1.
(8) Kausch, H. H. *Polymer Fracture*, Springer-Verlag: Heidelberg, Germany, 1978.
(9) Lauterwasser, B. D.; Kramer, E. J. *Philos. Mag.* **1979**, *A39*, 469.
(10) Brown, H. R. *J. Mater. Sci.* **1979**, *14*, 237.
(11) Donald, A. M.; Kramer, E. J. *Philos. Mag.* **1981**, *A43*, 857.
(12) Yang, A. C.-M.; Wang, R. C.; Lin, C. H. *Polymer* **1996**, *37*, 5751.
(13) Yang, A. C.-M.; Kramer, E. J.; Kuo C. C.; Phoenix, S. L. *Macromolecules* **1986**, *19*, 2010.
(14) Yang, A. C.-M.; Kramer, E. J.; Kuo C. C.; Phoenix, S. L. *Macromolecules* **1986**, *19*, 2020.
(15) Yang, A. C.-M.; Kunz, M. S.; Logan, J. A. *Macromolecules* **1993**, *26*, 1767.
(16) Yang, A. C.-M.; Wang, R. C.; Kunz, M. S.; Yang, I. C. *J. Polym. Sci.: Polym. Phys. Ed.* **1996**, *34*, 1141.
(17) Lin, C. H.; Yang, A. C.-M. *Macromolecules* **2001**, in press.
(18) Yang, A. C.-M.; Lee, C. K.; Ferline, S. *J. Polym. Sci.: Polym. Phys. Ed.* **1992**, *30*, 1123.
(19) Lin, C. H.; Yang, A. C.-M. *J. Mater. Sci.* **2000**, *35*, 4231.
(20) Donald, A. M.; Kramer, E. J.; Bubeck, R. A. *J. Polym. Sci.—Polym. Phys.* **1982**, *20*, 1129.
(21) Argon, A. S.; Salama, M. M. *Mater. Sci. Eng.* **1977**, *23*, 219.
(22) Taylor, G. I. *Proc. R. Soc. London* **1950**, *A201*, 192.
(23) Kramer, E. J. *Polym. Eng. Sci.* **1984**, *24*, 761.
(24) Berger, L. L.; Kramer, E. J. *Macromolecules* **1987**, *20*, 1980.
(25) Henkee, C. S.; Kramer, E. J. *J. Mater. Sci.* **1986**, *21*, 1398.
(26) Robertson, R. E. *J. Appl. Polym. Sci.* **1963**, *7*, 443.
(27) Brown, N.; Ward, I. M. *J. Polym. Sci. A-2* **1968**, *6*, 607.
(28) Ward, I. M. *J. Mater. Sci.* **1971**, *6*, 1397.
(29) Bucknall, C. B. *Toughened Plastics*; Applied Science: London, 1977.
(30) Ricco, T.; Pavan, A.; Danusso, F. *Polym. Eng. Sci.* **1978**, *18*, 774.
(31) Broutman, L. J.; Panizza, G. *Int. J. Polym. Mater.* **1971**, *1*, 95.
(32) Gregory, B. L.; Siegmann, A.; Im, J.; Hiltner, A.; Baer, E. *J. Mater. Sci.* **1987**, *22*, 532.
(33) Pan, S. J.; Im, J.; Hill, M. J.; Keller, A.; Hiltner, A.; Baer, E. *J. Polym. Sci., Part B: Polym. Phys.* **1990**, *28*, 1105.
(34) Ma, M.; Vijayan, K.; Hiltner, A.; IM, J.; Baer, E. *J. Mater. Sci.* **1990**, *25*, 2039.
(35) Shin, E.; Hiltner, A.; Baer, E. *J. Appl. Polym. Sci.* **1993**, *47*, 269.
(36) Haderski, D.; Sung, K.; Im, J.; Hiltner, A.; Baer, E. *J. Appl. Polym. Sci.* **1994**, *52*, 121.
(37) Sung, K.; Haderski, D.; Hiltner, A.; Baer, E. *J. Appl. Polym. Sci.* **1994**, *52*, 147.
(38) Zhu, C. X.; Umemoto, S.; Okui, N.; Sakai, T. *J. Mater. Sci.* **1988**, *23*, 4091.
(39) Zhu, C. X.; Umemoto, S.; Okui, N.; Sakai, T. *J. Mater. Sci.* **1989**, *24*, 2787.
(40) Berger, L. L.; Kramer, E. J. *J. Mater. Sci.* **1988**, *23*, 3536.
(41) Bridgman, D. W. *Studies in Large Plastic Flow and Fracture*; Harvard University Press: Cambridge, MA, 1964; p 9.
(42) Timoshenko, S. P.; Woinowsky-Krieger, S. *Theory of Plates and Shells*; McGraw-Hill International Ed.: New York, 1959.
(43) Hal, I. H. *J. Appl. Polym. Sci.* **1968**, *12*, 731.
(44) Wada, M.; Nakamura, T.; Kinoshita, N. *Philos. Mag.* **1978**, *A38*, 167.
(45) Whitlow, S. J.; Wool, R. P. *Macromolecules* **1989**, *22*, 2648.
(46) Lin, H. C.; Tsai, I. F.; Yang, A. C.-M.; Hsu, M. S.; Ling, Y. C. Submitted to *Macromolecules*.
(47) O'Neil, P. V. *Advanced Engineering Mathematics*; 2nd ed.; Wadworth Publishing Co.: 1987.
(48) Yang, A. C. M.; Ayala, J. E.; Scott, J. C. *J. Mater. Sci.* **1991**, *26*, 5823.
(49) de Gennes, P. G. *Scaling concept of polymer physics*; Cornell University Press: Ithaca, NY, 1979.

MA001586C